Electronic structure of carbosulfide superconductors

E. Z. Kurmaev, N. A. Skorikov, A. V. Galakhov, P. F. Karimov, V. R. Galakhov, V. A. Trofimova, and Yu. M. Yarmoshenko
Institute of Metal Physics, Russian Academy of Sciences, Ural Division, 620219 Yekaterinburg GSP-170, Russia

A. Moewes
Department of Physics and Engineering Physics, University of Saskatchewan, 116 Science Place, Saskatoon, Saskatchewan S7N 5E2, Canada

S. G. Chiuzbăian* and M. Neumann
Universität Osnabruck, Fachbereich Physik, D-49069 Osnabrück, Germany

K. Sakamaki
Japan Science and Technology Corporation (JST), 1-8 Honcyo 4-chome, Kawaguchi, Saitama 332-0012, Japan, National Institute for Materials Science, 1-1 Namiki, Tsukuba, Ibaraki 305-0044, Japan
(Received 18 February 2004; revised manuscript received 26 October 2004; published 28 January 2005)

We present electronic band structure calculations and x-ray emission and photoelectron measurements of the recently discovered van der Waals–type layered superconductors Nb_2S_2C and $Cu_{2/3}Nb_2S_2C$. Good agreement between our local partial density-of-states calculations and our experimental x-ray emission measurements of the constituents as well as between calculated and experimental $E(\mathbf{k})$ dispersion curves is found for Nb_2S_2C. For $Cu_{2/3}Nb_2S_2C$, we observe a strong interaction between Cu 3*d* and S 3*s*3*p* states that is responsible for shifting the S 3*s*3*p* states toward to the bottom of the valence band.

DOI: 10.1103/PhysRevB.71.024528 PACS number(s): 74.25.Jb, 74.72.Jt, 78.70.En, 78.70.Dm

I. INTRODUCTION

Layered transition-metal chalcogenides can be intercalated by a wide variety of guest atoms, which can modify their physical properties. Recently, layered structures with a periodical stacking sequence of sulfur–transition-metal–carbon–transition-metal–sulfur (M_2SC, $M_4S_2C_2$, and M_2S_2C, where M is a transition metal of groups IVa and Va) were discovered.[1–3] The $M_4S_2C_2$ carbosulfides of Ti and Zr are found to be hard compounds with a high chemical stability, which is comparable to the corresponding carbides.[4] On the other hand, M_2S_2C-type carbosulfides of Ta and Nb have a structure similar to transition-metal disulfides and, therefore, have a versatile host lattice for intercalation. The $[M_6C]$ octahedrons are separated by double layers of sulfur atoms, weakly bound by van der Waals forces. The nature of these bonds accounts for the softness of these materials, of which Ta_2S_2C has been proposed as a solid lubricant.[5] Nb_2S_2C could not be prepared by direct synthesis, and a topochemical reaction in conjunction with a chemical process is proposed to prepare this compound.[6,7] Recently a superconductivity with $T_c=7.6$ K was observed for Nb_2S_2C.[1] The Cu-intercalated Nb_2S_2C compound ($Cu_{2/3}Nb_2C$) has shown a reduction of superconducting transition temperature to 4.85 K.[3] In the present paper we have studied the electronic structure of Nb_2S_2C and $Cu_{2/3}Nb_2S_2C$ using first-principles band structure calculations and x-ray emission and photoelectron emission measurements.

II. EXPERIMENTAL AND CALCULATION DETAILS

$Cu_{2/3}Nb_2S_2C$ was synthesized by conventional vacuum sintering using appropriate amounts of Nb_2SC, S, and 2/3 Cu and sintering at 1200 °C for 30 days. Nb_2S_2C was prepared by stirring $Cu_{2/3}Nb_2S_2C$ in 0.2 mol/l iodine dehydrated acetonitrile solution for 7 days in a nitrogen flow glove box at room temperature. Nb_2S_2C was filtered out under reduced pressure, rinsed with dehydrated acetonitrile, and then dried under vacuum at about 1000 °C for more than 5 h. Further synthesis details are given in Ref. 3. According to x-ray diffraction (XRD) data, $Cu_{2/3}Nb_2S_2C$ has 1*T*-type structure with lattice parameters $a=3.3168(2)$ Å and $c=9.0245(3)$ Å, whereas XRD data of Nb_2S_2C are a superposition of 1*T* and 3*R*-type structures (1*T*, 76 wt % and 3*R*, 24 wt %).[3] Nb_2S_2C and $Cu_{2/3}Nb_2S_2C$ are found to be superconducting at 7.6 and 4.85 K, respectively.

The soft x-ray fluorescence measurements of Nb_2S_2C and $Cu_{2/3}Nb_2S_2C$ were performed at Beamline 8.0.1 of the Advanced Light Source at Lawrence Berkeley National Laboratory employing the soft x-ray fluorescence endstation.[8] The emitted radiation was measured using a Rowland-circle-type spectrometer with large spherical gratings and a multichannel two-dimensional detector. The spectrometer resolution at the C 1*s*, S 2*p*, and Cu 2*p* thresholds is about 0.4, 0.4, and 1.8 eV, respectively. The energies of the incident photons for carbon $K\alpha$ ($2p\rightarrow 1s$ transition), S $L_{2,3}$ ($3s$, $3d\rightarrow 2p$ transition), and Cu $L\alpha,\beta$ ($3d$, $4s\rightarrow 2p$ transition) x-ray emission spectra (XES) were 300, 230, and 960 eV, respectively. Resonant inelastic x-ray scattering spectra (RIXS) were measured at the carbon *K* edge.

The Nb $L\beta_{2,15}$ ($4d$, $5s\rightarrow 2p$ transition) and S $K\beta_{1,3}$ ($3p\rightarrow 1s$ transition) x-ray emission spectra were measured using a fluorescent Johan-type vacuum spectrometer with a position-sensitive detector.[9] The palladium $K\alpha$ x-ray radiation from an x-ray tube was used to excite the fluorescent S $K\beta_{1,3}$ spectra. A quartz (1010) single crystal curved to *R*

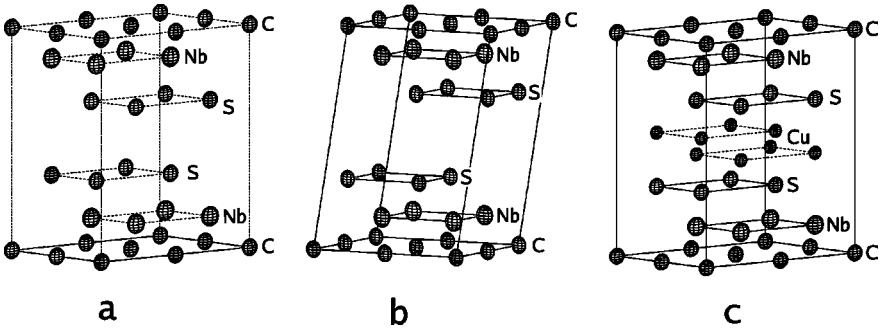

FIG. 1. Crystal structure of $1T$-Nb_2S_2C (a), $3R$-Nb_2S_2C (b), and $1T$-$Cu_{2/3}Nb_2S_2C$ (c) phases.

=1400 mm served to disperse the radiation. The spectra were measured with an energy resolution of approximately 0.3–0.4 eV, and the x-ray tube was operated at $V=25$ keV, $I=50$ mA.

The x-ray photoelectron spectra (XPS) were measured using an ESCA spectrometer from Physical Electronics (PHI 5600 ci) with monochromatic Al $K\alpha$ radiation. The pressure in the vacuum chamber during the measurements was below 5×10^{-9} mbar. Prior to the XPS measurements, the samples were fractured in ultrahigh vacuum. The XPS spectra were calibrated using an Au foil to obtain photoelectrons from the Au $4f_{7/2}$ subshell (binding energy of 84.0 eV).

In order to calculate the band structure of Nb_2S_2C and $Cu_{2/3}Nb_2S_2C$, we have used the self-consistent tight-binding (TB) linear muffin-tin orbitals method (LMTO) in the atomic sphere approximation (ASA). Calculations were carried out using the TB-LMTO-ASA code (version 47).[10] Atomic coordinates of Nb, S, and C of $1T$-Nb_2S_2C [$2d$ **(**1/3,2/3, 0.141(3)**)**, $2d$ **(**1/3,2/3,0664(9)**)**, and $1a$ (0,0,0)], $3R$-Nb_2S_2C [$6c$ **(**0,0,0.379(2)**)**, $6c$ **(**0,0,0.229(6)**)**, and $3a$ (0,0,0)], and atomic coordinates of Cu, Nb, S, and C of $1T$-$Cu_{2/3}Nb_2S_2C$ [$2d$ **(**1/32/3,0.453(5)**)**, $2d$ **(**1/3,2/3, 0.127(2)**)**, $2d$ **(**1/3,2/3,0.689(2)**)**, and $1a$ (0,0,0)] were taken from Ref. 3. Structures are shown in Fig. 1.

III. RESULTS AND DISCUSSION

Since the sample of Nb_2S_2C is a mixture of $1T$ and $3R$ phases, we have simulated its electronic structure as a sum of the electronic structures, calculated for both phases taken in the relation $0.76(1T)+0.24(3R)$. Figure 2 shows total densities of states for pure phases and their weighted sum. As one can see, the DOS weakly depends on the crystal structure.

The calculated electronic band structures of Nb_2S_2C (wighted sum of $1T$ and $3R$ phases) and $Cu_{2/3}Nb_2S_2C$ are given in Figs. 3 and 4. The Nb $L\beta_{2,15}$, S $L_{2,3}$, S $K\beta_1$, and C $K\alpha$ XES, which probe Nb $4d$, S $3s$, S $3p$, and C $2p$ states, respectively, are converted to the binding energy scale using core-level XPS measurements. The data are compared with calculated partial density of states (DOS) in the same figures and show good agreement between theory and experiment.

The total DOS curves show metallic like features with density of states at the Fermi level $N(E_F)$ of 0.94 and 1.87 states eV^{-1} (unit cell)$^{-1}$ for Nb_2S_2C and $Cu_{2/3}Nb_2S_2C$, respectively, which agrees with Ref. 3 where charge transfer from Cu to Nb_2S_2C and an increase in conduction electrons are suggested. Based on these calculations, the electronic states at the top of the valence band of Nb_2S_2C (Fig. 3) are formed by Nb $4d$ and S $3p$ states. C $2p$ states are located at the bottom of the valence band, and S $3p$ and C $2p$ states are separated by an energy gap of about 4 eV and show atomiclike features.

Using RIXS at the carbon $1s$ edge, we have carried out quantitative band mapping and compared calculated and experimental dispersion bands. In the band mapping procedure,[11] the excitation energies (E_{exc}) are selected at features labeled *a*-*d* in the absorption spectrum (Fig. 5), which correspond to points of high symmetry in the Brillouin zone. Carbon $K\alpha$ XES were measured for selected excitation energies through the C $1s$ threshold and the emission spectra were normalized to the incident flux (Fig. 6) monitored by a transparent gold mesh.

In order to reconstruct the dispersion curves experimentally from the resonant emission spectra, we have used an established procedure for example described in Ref. 12. In Fig. 5 we compare carbon $K\alpha$ emission and $1s$ absorption of Nb_2S_2C with our total DOS calculations made for the mixture of $1T$ and $3R$ phases. The top of the C $K\alpha$ emission band ($E=282.6$ eV) corresponds to zero on the calculated energy scale. The possible values for the **k** vector for excited C $1s$ electrons are determined by intersecting horizontal lines that correspond to the selected excitation energies and the calcu-

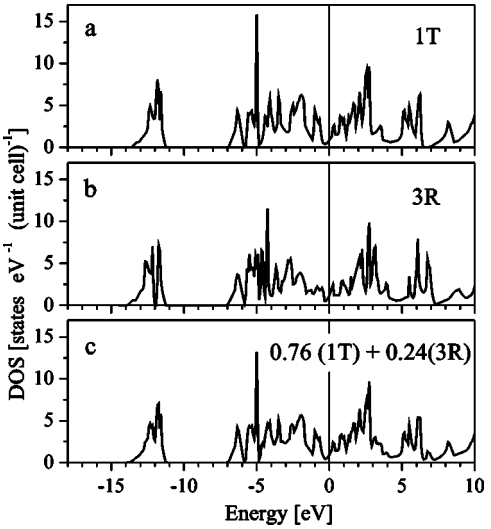

FIG. 2. Total densities of states of Nb_2S_2C calculated for $1T$ and $3R$ phases and as a weighted sum of $1T$ and $3R$ phases taken in the relation $0.76(1T)+0.24(3R)$.

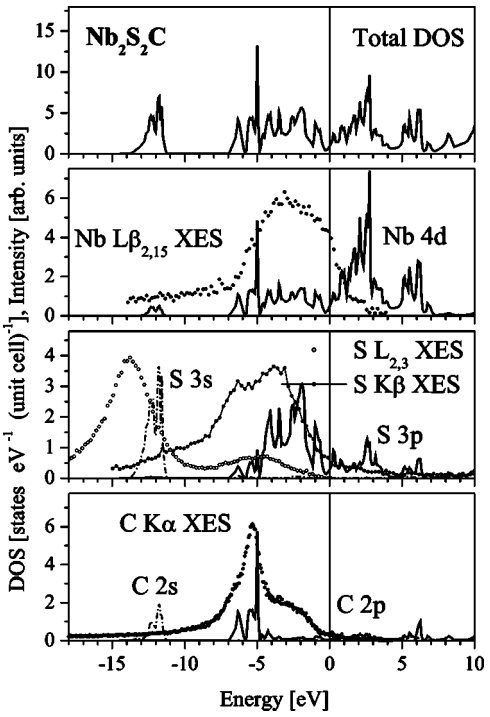

FIG. 3. Total and partial density of states of Nb_2S_2C (solid and dashed lines), Nb $L\beta_{2,15}$, S $L_{2,3}$, S $K\beta$, and C $K\alpha$ XES.

lated dispersion curves for 2*p* vacant states (see, for example, the solid horizontal line in Fig. 7, corresponding to an excitation energy of 282.6 eV that intersects the dispersion curves of the unoccupied states in three points).

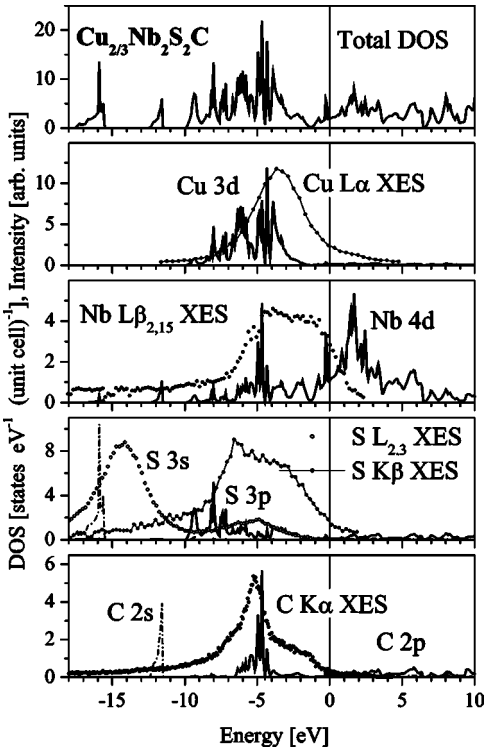

FIG. 4. Total and partial density of states of $Cu_{2/3}Nb_2S_2C$ (solid and dotted lines), Cu $L\alpha$, Nb $L\beta_{2,15}$, S $L_{2,3}$, S $K\beta$, and C $K\alpha$ XES.

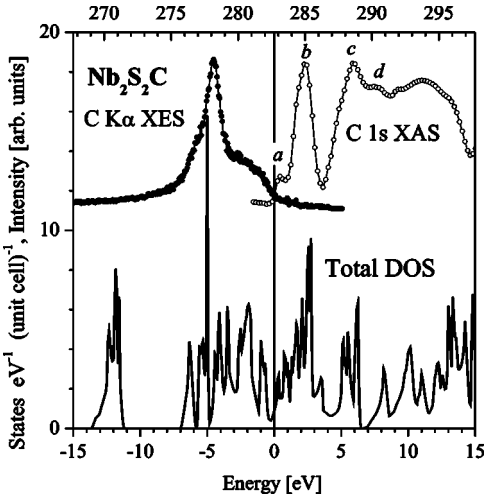

FIG. 5. C $K\alpha$ x-ray emission and C 1*s* x-ray absorption spectra and total density of states of Nb_2S_2C.

Following the idea of **k** momentum conservation, vertical lines from these intersection points are drawn to the dispersion curves for the occupied states from where the subsequent radiative decay will occur (see the vertical lines in Fig. 7). The energy positions of these occupied states correspond to the energy positions of features in the carbon $K\alpha$ emission spectrum for each selected excitation energy (see Fig. 6), and the points where vertical and horizontal dotted lines intersect are represented by the symbols in Fig. 7. The same procedure is used for each carbon $K\alpha$ emission spectrum and different symbols represent different excitation energies. The obtained results agree well with the calculated dispersion curves for Nb_2S_2C (Fig. 7).

One can see from Figs. 3 and 4 that introducing Cu to Nb_2S_2C results in changes most noticeably in the sulfur energy bands: S 3*s* states shift to lower energies and away from the top of the valence band (about 4.1 eV). S 3*p* and Nb 4*d*

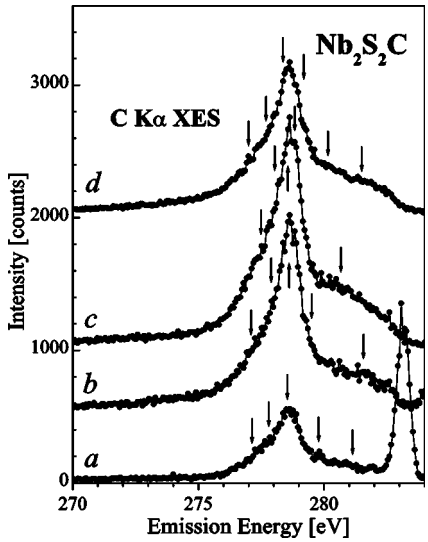

FIG. 6. C $K\alpha$ x-ray emission spectra of Nb_2S_2C measured at excitation energies of 283.1 eV (curve *a*), 285.0 eV (curve *b*), 288.5 eV (Curve *c*), and 290.5 eV (curve *d*).

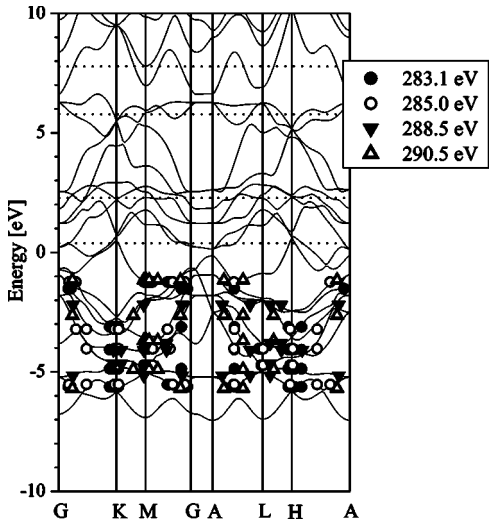

FIG. 7. Comparison of calculated and experimental dispersion curves based on the analysis of the C $K\alpha$ x-ray emission spectra of Nb_2S_2C measured at excitation energies of 283.1, 285.0, 288.5, and 290.5 eV.

states are split and reside about 3 eV higher. The C 2*p* states are slightly shifted toward the top of the valence band (by about 0.5 eV). We note that in undoped Nb_2S_2C the S 3*p* and Nb 4*d* states reside in almost the same energy range through almost the entire valence band whereas the C 2*p* states are situated close to the bottom of the valence band.

The insertion of Cu 3*d* states (near the center of the valence band) therefore strongly affects the electronic structure of Nb_2S_2C, pushing S 3*s* and S 3*p* states out of the Cu 3*d* band energy. Such behavior was observed also in ternary copper tellurides and selenides and is discussed in terms of the *d-sp* resonance model.[13] Based on our findings we can conclude that a strong interaction between Cu 3*d* and S 3*s*, 3*p* states takes place in $Cu_{2/3}Nb_2S_2C$ which enhances the interaction between layers and can be reason for reduction of superconductivity in Nb_2S_2C. It was shown in Ref. 14 that a strong interaction with iron-impurities between layers in iron-doped TaS_2 reduces the superconducting transition temperature.

In Fig. 8 nonresonant Cu $L\alpha$, β XES of $Cu_{2/3}Nb_2S_2C$ are compared with spectra of Cu metal and reference compounds of different valence, $CuIr_2S_4$ (Cu^+, metal conductivity) and CuO (Cu^{2+}, insulator). The intensity ratio $I(L\beta)/I(L\alpha)$ is small for pure metal and deviates from the value of 0.5 expected due to the $j=3/2$ and $j=1/2$ occupancy ratios. This is a result of $L_2L_3M_{4,5}$ Coster-Kronig (CK) processes.[15] It is further known that the $I(L\beta)/I(L\alpha)$ intensity ratio increases from pure 3*d* metals to their oxides because the nonradiative $L_2L_3M_{4,5}$ CK transition probability is expected to be lower for 3*d* oxides than for metals. Reference 16 suggests that one of the CK channels is due to excitation of free carriers and this channel is largely suppressed in metals. The intensity ratio $I(L\beta)/I(L\alpha)$ for $Cu_{2/3}Nb_2S_2C$ is small and comparable with that for pure Cu metal since the Cu-intercalated carbosulfide is characterized by metallic conductivity and, therefore, a decrease of number of carriers leads to disconnection of the CK channel.

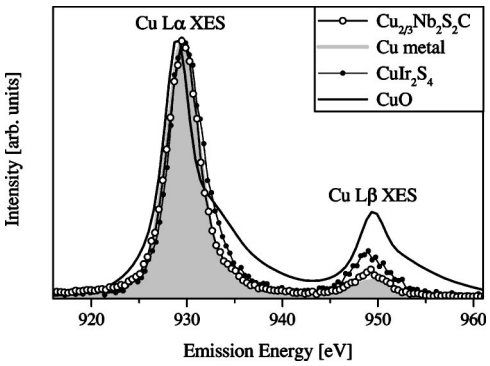

FIG. 8. Cu $L\alpha$, β emission spectra of a carbosulfide, $Cu_{2/3}Nb_2S_2C$, and reference compounds Cu metal (solid area), $CuIr_2S_4$, and CuO.

According to our band structure calculations, the density of states at the Fermi level is 1.18 states/(eV cell) for 1*T*-Nb_2S_2C, 1.60 states/(eV cell) for 3*R*-Nb_2S_2C, and 1.97 states/(eV cell) for $Cu_{2/3}Nb_2S_2C$. Based on these values one would therefore expect higher T_c values for $Cu_{2/3}Nb_2S_2C$ than for Nb_2S_2C but the experiments show the opposite behavior: $T_c=7.6$ K for Nb_2S_2C and $T_c=4.85$ K for $Cu_{2/3}Nb_2S_2C$.[3] The decrease in T_c for Cu-doped Nb_2S_2C does not correlate with the decrease of the density of states at the Fermi level and could be explained by intercalation of Cu atoms between the layers. This intercalation results in reduction of the two dimensionality of the compound, which is known to be one of the favorable conditions for superconductivity.

IV. CONCLUSION

In conclusion, we have studied the electronic structure of van der Waals–type layered superconductors Nb_2S_2C and $Cu_{2/3}Nb_2S_2C$ by means of x-ray photoelectron emission and resonant emission spectroscopy and compared with our band structure calculations. We find good agreement between the partial density of state calculations and the measured x-ray emission spectra of the constituents as well as between calculated and experimental $E(\mathbf{k})$ dispersion curves for Nb_2S_2C. For $Cu_{2/3}Nb_2S_2C$, the strong interaction between Cu 3*d* and S 3*s*3*p* states pushes the S 3*s*3*p* states out of the Cu 3*d* band energy. Inserting of Cu into Nb_2S_2C induces a strong interaction between layers that reduces the two dimensionality of this compound and leads to a decrease of T_c.

ACKNOWLEDGMENTS

Funding by the Research Council of the President of Russian Federation (Project No. NSH-1026.2003.2), Russian Ministry for Industry and Science (Project on Superconductivity of Mesoscopic and Strongly Correlated Systems), and the Natural Sciences and Engineering Research Council of Canada (NSERC) is gratefully acknowledged. The work at the Advanced Light Source at Lawrence Berkeley National Laboratory was supported by the U.S. Department of Energy (Contract No. DE-AC03-76SF00098). One of the authors (V.R.G.) gratefully acknowledges support from the Deutscher Akademischer Austauschdienst (DAAD) Program.

*Present address: Paul Scherrer Institut, Swiss Light Source, CH-5232 Villigen, Switzerland.

[1] K. Sakamaki, H. Wada, H. Nozaki, Y. Onuki, and M. Kawai, Solid State Commun. **112**, 323 (1999).
[2] J. Walter, W. Boonchuduang, and S. Hara, J. Alloys Compd. **305**, 259 (2000).
[3] K. Sakamaki, H. Wada, H. Nozaki, Y. Onuki, and M. Kawai, Solid State Commun. **118**, 113 (2001).
[4] C. Frick and H. Rohde, Arch. Eisenhuettenwes. **31**, 419 (1960).
[5] O. Beckmann, H. Boller, and H. Nowotny, Monatsch. Chem. **101**, 945 (1970).
[6] H. Boller and K. Hiebl, J. Alloys Compd. **183**, 438 (1992).
[7] K. Sakamaki, H. Wada, H. Nozaki, Y. Onuki, and M. Kawai, J. Alloys Compd. **339**, 283 (2002).
[8] J. J. Jia, T. A. Callcott, J. Yurkas, A. W. Ellis, F. J. Himpsel, M. G. Samant, J. Stohr, D. L. Ederer, J. A. Carlise, E. A. Hudson, L. J. Terminello, D. K. Shuh, and R. C. C. Perera, Rev. Sci. Instrum. **66**, 1394 (1995).
[9] V. E. Dolgih, V. M. Cherkashenko, E. Z. Kurmaev, D. A. Goganov, E. K. Ovchinnikov and Yu. M. Yarmoshenko, Nucl. Instrum. Methods Phys. Res. A **224**, 117 (1984).
[10] M. Methfessel, M. van Schilfgaarde, and R. A. Casali, in *Electronic Structure and Physical Properties of Solids: The Use of the LMTO Method*, edited by H. Dreysse, Lecture Notes in Physics, Vol. 535 (Springer-Verlag, Berlin, 2000).
[11] S. Eisebitt and W. Eberhardt, J. Electron Spectrosc. Relat. Phenom. **110–111**, 335 (2000).
[12] A. V. Sokolov, E. Z. Kurmaev, S. Leitch, A. Moewes, J. Kortus, L. D. Finkelstein, N. A. Skorikov, C. Xiao, and A. Hirose, J. Phys.: Condens. Matter **15**, 2081 (2003).
[13] E. P. Domashevskaya, V. V. Gorbachev, V. A. Terekhov, V. M. Kashkarov, E. V. Panfilova, and A. V. Shchukarev, J. Electron Spectrosc. Relat. Phenom. **114–116**, 901 (2001).
[14] R. M. Fleming and R. V. Coleman, Phys. Rev. Lett. **34**, 1502 (1975).
[15] H. W. B. Skinner, T. G. Bullen, and J. Jonston, Philos. Mag. **45**, 1070 (1954).
[16] V. I. Grebennikov, Surface Investigations: X-ray, Synchrotron and Neutron Techniques, No. 11, 41 (2002).